Leading Surface Optimization Criteria for Orbital Lifting Re-Entry Craft

LAWRENCE E. HOOKS*
Ohio State University, Columbus, Ohio

AND

WILBUR L. HANKEY JR.†
Wright-Patterson Air Force Base, Ohio

Nose and leading-edge surfaces for orbital lifting re-entry craft are examined in hypersonic flow. General selection criteria are established for optimizing the surface for two design situations: 1) minimizing heating rate for fixed drag, and 2) minimizing drag for a given heating rate. A parametric study of elliptical leading surfaces (two- and three-dimensional) shows that an ellipticity of about 0.45 produces the desired optima. Reductions in drag up to 65% are found at the appropriate minima for the optimum ellipticity. The influence of angle-of-attack modulation is also considered for leading edges.

Nomenclature

A = area
a = elliptical semiaxis parallel to freestream flow
b = elliptical semiaxis perpendicular to freestream flow
C_D = pressure drag coefficient based on frontal area
h = enthalpy
$(L/D)_{max}$ = maximum lift-to-drag ratio
m = exponent in Eq. (6)
n = zero for a two-dimensional body, one for a body of revolution
P = local static pressure
$\overline{Pr}$ = average Prandtl number
q = local heat-transfer rate per unit area
R = local radius of curvature
R_0 = gas constant
S = dimensional distance along body surface from stagnation point
s = S/R_s
T = absolute temperature
V = local inviscid gas velocity, tangent to the body surface when freestream conditions are indicated
X = dimensional distance along body axis from stagnation point
Y = dimensional distance from body axis to body surface
y = Y/R_s
α = vehicle angle of attack
α_e = leading-edge effective angle of attack
α_{opt} = vehicle angle of attack at $(L/D)_{max}$
β = $[(\gamma - 1)/\gamma]^{1/2}$
γ = effective ratio of specific heats in the shock layer
θ = angle between tangent plane at local body point and tangent plane at stagnation point
Λ = sweep angle
μ = absolute viscosity
ρ = density
ω = μ/R_0T

Subscripts

A = constant base area
b = quantities related to base of body
c = circular cross-section body
D = constant drag
e = elliptical cross-section body
p = peak heating rate
q = constant heating rate
s = stagnation-point conditions
δ = conditions at outer edge of the boundary layer
1, 2 = body index numbers
$2D$ = leading edge
$3D$ = nose
∞ = freestream conditions

Received May 25, 1964; revision received December 3, 1964. The work reported here was carried out at the Flight Dynamics Laboratory, Wright-Patterson Air Force Base, Ohio.

* Research Associate, Department of Aeronautical and Astronautical Engineering; formerly Physicist, Flight Dynamics Laboratory, Wright-Patterson Air Force Base, Ohio. Member AIAA.

† Research Aerospace Engineer, Hypersonic Research Laboratory, Aerospace Research Laboratories. Member AIAA.

Introduction

AT hypersonic speeds, the pressure drag on the nose and leading edge of a lifting re-entry vehicle represents a sizeable part of the total vehicle drag. The nondimensional pressure distributions on these surfaces essentially depend only on attitude for a given vehicle geometry, so the designer may use the hypersonic pressure drag coefficient as a measure of efficiency when choosing low-drag fore-surface contours. Since leading-edge and nose surfaces are also critical heating areas, the designer must limit his goal of minimizing leading-surface pressure drag by the requirement that the peak heating rate on these surfaces be held to a tolerable value.

Present indications are that radiation heating is negligible at orbital velocities for lifting re-entry craft and that the boundary layers on their leading surfaces will be laminar during the re-entry heating pulse. For constant-surface geometry, pressure drag decreases with decreasing size, but laminar convective heating rates increase. Leading surfaces of any shape should thus be as small as possible to reduce drag while still sustaining the peak heating rate to be experienced. Nondimensional laminar heating distributions with a common nondimensionalizing factor may be used to compare leading-surface heating characteristics in the same way that drag coefficients grade surfaces for low-drag characteristics in hypersonic flight.

Assuming that the surfaces considered are cooled solely by equilibrium reradiation during the orbital heating pulse, the surface material temperature limit corresponds to a unique local heat-transfer limit.[1] The maximum value of nondimensional heating distribution is critical in this situation whether it occurs at the stagnation point or elsewhere. If the designer is satisfied with existing vehicle performance reflected by existing nose and leading-edge drag, maximum freedom in vehicle trajectory may be obtained by choosing leading surfaces that give the minimum value of critical local heating rate while not exceeding the given drag. Al-

ternately, if the designer has a material temperature constraint, the leading surfaces chosen should be those that have minimum pressure drag while sustaining the peak temperature expected. Thus, two mathematical problems may arise: 1) minimizing temperature for a fixed total drag, or 2) minimizing drag for a given temperature limit.

Hypersonic pressure drag coefficients and nondimensional laminar heating distributions have been computed on an IBM 7090 for ellipsoid-of-revolution noses and elliptical-cylinder leading edges. Based on these results, elliptical noses and leading edges are compared in this paper according to the aforementioned criteria. Although the optimal elliptical shapes do not represent absolute optimum surfaces, they are shown to be marked improvements over circular shapes according to both criteria. In addition, the characteristics of the two families of elliptical shapes provide an excellent standard with which to compare other leading-surface contours.

Convective Heating-Rate Distribution

Lees[2] describes the convective heat-transfer distribution near the stagnation point of a blunt body in hypersonic flight by

$$\frac{q}{q_s} = \frac{(P/P_s)(\omega_\delta/\omega_s)(V_\delta/V_\infty)Y^n}{\left[\frac{2^{n+1}}{R_s}\left(\frac{R}{V_\infty}\frac{dV_\delta}{dS}\right)_s \int_0^s \frac{P}{P_s}\frac{\omega_\delta}{\omega_s}\frac{V_\delta}{V_\infty} Y^{2n}\, dS\right]^{1/2}} \quad (1)$$

where $n = 0$ for a two-dimensional body, and $n = 1$ for a body of revolution. In developing Eq. (1), it was assumed that a) heating due to shock-layer radiation may be neglected, b) the boundary layer and shock wave are distinct, and c) the enthalpy gradient at the surface is given by $0.47\ (\overline{Pr})^{1/3}$ and the surface heat-transfer-rate distribution is obtained directly from the surface pressure distribution. When it is assumed that 1) the static pressure distribution is modified Newtonian, 2) the total pressure along an inviscid streamline is equal to the stagnation-point value, 3) $h_s = V_\infty^2/2$, and 4) $\omega_\delta/\omega_s = 1$, and, when Y and S are nondimensionalized by R_s, Eq. (1) becomes[1]

$$\frac{q}{q_s} = \frac{\cos^2\theta(1 - \cos^{2\beta^2}\theta)^{1/2} y^n}{\left[2^{n+1}\beta \int_0^\theta \cos^2\phi(1 - \cos^{2\beta^2}\phi)^{1/2}\, y^{2n} \frac{ds}{d\phi}\, d\phi\right]^{1/2}} \quad (2)$$

where ϕ is the dummy variable for θ. For a given nose or leading-edge geometry, $s(\theta)$ and $y(\theta)$ form a unique functional pair so that $q(\theta)/q_s$ as given in Eq. (2) depends only on body shape and effective γ in the shock layer. Specifically, $q(\theta)/q_s$ does not depend on body size. Thus, the absolute magnitude of laminar heating rate at similar locations on geometrically similar shapes at the same flight conditions varies in exactly the same manner with body size as the stagnation-point heating rate. To the extent that γ may be considered constant between two cases being compared, $q(\theta)$ also varies with ρ_∞ and V_∞ in the same way as q_s.

Turning to the stagnation point of a noncircular body, the heating rate may be represented by

$$q_s = 2^{n/2} f(\rho_\infty, V_\infty) R_b^{-1/2} (R_s/R_b)^{-1/2} \quad (3)$$

where R_b is the base radius and R_s/R_b is the ratio of stagnation-point radius of curvature to base radius. Thus, q_s is dependent on body size and body geometry.

Consider two bodies, indexed 1 and 2, in laminar flow at the same V_∞ and ρ_∞ with the same n. Let the point of interest on body 1 be the peak heating point. Let body 2 be a circular cross-sectional body, and choose the stagnation point as the point of interest on that body. With these conditions

$$q_{1p}/q_{cs} = (q_{1p}/q_{1s})(R_{cb}/R_{1b})^{1/2}(R_{1b}/R_{1s})^{1/2} \quad (4)$$

since $(q_s/q_s)_c = 1$ and $R_{cs}/R_{cb} = 1$. It is convenient to nondimensionalize the peak heating rate on body 1 by the stagnation heating rate of a circular cross-sectional body with the same base radius (and area). Then

$$q_{1p}/q_{cs} = (q_{1p}/q_{cs})_A (R_{cb}/R_{1b})^{1/2} \quad (5)$$

Leading Surface Selection Criteria

The ratio of the drag forces on two bodies at the same flight condition, hence, the same dynamic pressure, is given by the ratio of their C_DA products. Multiplying Eq. (5) by these drag equalities gives

$$\frac{D_1}{D_c}\left(\frac{q_{1p}}{q_{cs}}\right)^m = \frac{C_{D1}}{C_{Dc}}\left(\frac{q_{1p}}{q_{cs}}\right)^m_A \frac{A_1}{A_c}\left(\frac{R_{cb}}{R_{1b}}\right)^{m/2} \quad (6)$$

Each term of Eq. (5) was raised to the mth power before multiplication to provide a controllable variable in Eq. (6). The exponent m is adjusted to eliminate A_1, A_c, R_{b1}, and R_{bc}. If nose and leading-edge total drag are constrained for a given design, the designer may minimize peak convective heating rate, i.e., he may minimize q_{1p}/q_{cs} with $D_1 = D_c$.

For unit lengths of two leading edges, the base areas are given by $A_1 = 2R_{b1}$ and $A_c = 2R_{bc}$. Letting $m = 2$, Eq. (6) gives

$$2D \qquad (q_{1p}/q_{cs})_{D2D} = (C_{D1}/C_{Dc})^{1/2}(q_{1p}/q_{cs})_A \quad (7)$$

as the quantity to be minimized. For noses with circular bases, $A_1 = \pi R_{1b}^2$ and $A_c = \pi R_{cb}^2$. Letting $m = 4$, Eq. (6) gives

$$3D \qquad (q_{1p}/q_{cs})_{D3D} = (C_{D1}/C_{Dc})^{1/4}(q_{1p}/q_{cs})_A \quad (8)$$

In a practical design problem, the circular cross-section surface is first sized by material limits and mission requirements. Then, the test surface size is determined by the requirement that $D_1 = D_c$. The expression just obtained is thus an equation for comparing peak heating rates on different sized surfaces related by equality of drag force. For example, if a nose has $(q_{1p}/q_{cs})_{D3D} = 0.75$, the peak heating rate on that nose at a given flight condition will be 75% of the peak heating on a hemisphere nose at the same flight condition when the two noses are sized to have the same hypersonic drag.

Alternatively, if the nose and leading-edge temperature limits are constrained, the designer may wish to minimize drag. The relationships for evaluating the efficiency of shapes by this criterion are found by setting $q_{1p} = q_{cs}$ in Eq. (6) and minimizing D_1/D_c:

$$2D \qquad (D_1/D_c)_{q2D} = (C_{D1}/C_{Dc})(q_{1p}/q_{cs})^2_A \quad (9)$$

$$3D \qquad (D_1/D_c)_{q3D} = (C_{D1}/C_{Dc})(q_{1p}/q_{cs})^4_A \quad (10)$$

Elliptical Cross-Sectional Shapes

A parametric study of elliptical leading edges and noses is discussed in this section to illustrate the use of Eqs. (7–10). Elliptical geometry was chosen, since it provides a single parameter family of shapes (a/b, the ellipticity) varying from very blunt through circular to sharp. In addition, elliptical leading surfaces may be fitted to the remainder of the vehicle without creating unrounded junctures. Consider the elliptical equation

$$(X^2/a^2) + (Y^2/b^2) = 1 \quad (11)$$

where X and Y are Cartesian axes for the leading edge and cylindrical axes for the noses. X is chosen as the axis of symmetry for noses and the plane of symmetry for leading edges. The nose or leading-edge angle of attack will be 0° when the stagnation point or line falls on the intersection of the X axis and the elliptical surface. The nose or leading-edge angle of attack may be different than the vehicle angle

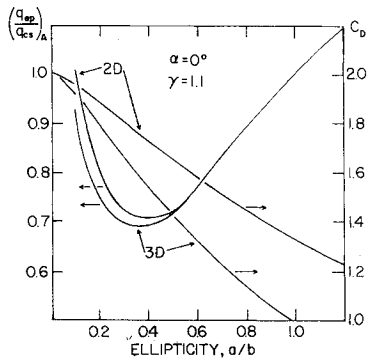

Fig. 1 Drag coefficients and peak heating rates on elliptical surfaces.

of attack because of orientation of the leading surfaces. Let θ be the angle between the local surface normal and the freestream velocity vector. Define θ positive in the direction of increasing Y:

$$\cot\theta = \pm(b^2/a^2)(X/Y) \tag{12}$$

$$Y = \pm(b^2 \tan\theta)/(a^2 + b^2 \tan^2\theta)^{1/2} \tag{13}$$

$$dS/d\theta = (a^2b^2 \sec^3\theta)/(a^2 + b^2 \tan^2\theta)^{3/2} \tag{14}$$

The pressure drag is defined here as

$$D = \int P \cos\phi(dA/d\phi)\, d\phi \tag{15}$$

where ϕ is the dummy variable for θ, and $\cos\phi$ selects the component of P parallel to V_∞. Base pressure is assumed to be negligible. Substituting the Newtonian approximation for hypersonic flight (P_s is twice the dynamic pressure) and using the base area A_b as the reference area gives $D = C_D A_b P_s/2$.

Noses and leading edges are considered to terminate at $X = 0$, $Y = \pm b$, or $\theta = \pm 90°$ when the surface angle of attack is 0°, and leading-edge cases are based on unit length of unswept leading edge. The base areas are thus $A_{2D} = 2b$ and $A_{3D} = \pi b^2$. Inserting the relations $(dA/d\phi)_{2D} = dS/d\phi$ and $(dA/d\phi)_{3D} = 2\pi Y(dS/d\phi)$ in Eq. (15) gives

$$C_{D2D} = \int_{-\pi/2}^{\pi/2} \frac{P}{P_s} \cos\phi \frac{d(S/b)}{d\phi}\, d\phi \tag{16}$$

and

$$C_{D3D} = 4 \int_0^{\pi/2} \frac{P}{P_s} \cos\phi \frac{Y}{b} \frac{d(S/b)}{d\phi}\, d\phi \tag{17}$$

Equations (16) and (17) were solved with $P/P_s = \cos^2\theta$ for a/b between 0.1 and 1.2 and $\alpha = 0°$. Figure 1 shows the results that provide one of the two terms on the right sides of Eqs. (7–10). The second term required in each equation was computed from

$$(q_{ep}/q_{cs})_A = (q_{ep}/q_{cs})(R_{eb}/R_{es})^{1/2} \tag{18}$$

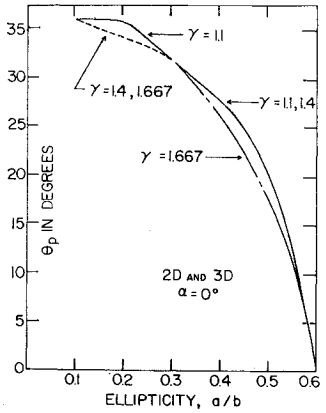

Fig. 2 Angular locations of peak heating rates on elliptical surfaces.

Setting $\theta = 0$ in Eq. (14) gives the stagnation-point radius of curvature as

$$(dS/d\theta) = b^2/a = R_{es} \qquad \theta = 0 \tag{19}$$

Now $R_{eb} = b$, so that

$$R_{eb}/R_{es} = a/b \tag{20}$$

$(q_{ep}/q_{cs})_A$ was then found as a function of a/b by computing $q_e(\theta)/q_{es}$ from Eqs. (2, 13, and 14), selecting the peak value of $q_e(\theta)/q_{es}$, and multiplying by $(a/b)^{1/2}$. This procedure was carried out for $n = 0, 1$; a/b between 0.1 and 1.2; $\alpha = 0°$; and $\gamma = 1.1$. Figure 1 also shows the results of these calculations.

It was found that the location of the peak heating point moved away from the stagnation point with decreasing a/b. Figure 2 shows this effect.

Combining the drag and heating results in Fig. 1 in Eqs. (7–10) gives values for $(q_{ep}/q_{es})_{D2D}$, $(q_{ep}/q_{cs})_{D3D}$, $(D_e/D_c)_{q2D}$, and $(D_e/D_c)_{q3D}$ as functions of a/b. These curves are shown in Figs. 3 and 4. As an indication of the validity of the aforementioned computations, the selection-criteria values have been computed using Vinokur's constant-density computations for elliptical noses.[3] These results are also shown in Figs. 3 and 4.

A value of $\gamma = 1.1$ was used in the present computations to provide formal agreement with Vinokur's work. Check calculations showed an increase in the effect of γ in Eq. (2) as ellipticity decreased. For an ellipticity of 0.2, q_{ep}/q_{cs} increases less than 3%, for either nose or leading edge, as γ varies from 1.1–1.667. Therefore, the information presented in this paper is effectively independent of γ.

Values of the present selection criteria for the constant heating-rate (*CHR*) surfaces of Ref. 1 are displayed in Figs. 3 and 4. Drag and heating computations for these surfaces were made in the same manner as those previously described for elliptical surfaces.

Extensive data have demonstrated that the modified Newtonian pressure distribution is an extremely good approximation for spheres in hypersonic flow. It is also accepted that the constant-density approximation is valid for flat-nosed cylinders in hypersonic flow. It is reasonable to assume, then, that the modified Newtonian and constant-density values of $(q_{ep}/q_{cs})_D$ and $(D_e/D_c)_q$ given in Figs. 3 and 4 represent limits on these values for noses intermediate in bluntness between spheres and flat-nosed cylinders.

Angle-of-Attack Effects

The optimized forecomponent configurations should be oriented on the lifting vehicle to produce their best results at $(L/D)_{max}$; the minor axis (X) of the nose should parallel the velocity vector at α_{opt} [vehicle angle of attack for $(L/D)_{max}$], and the minor axis of the leading edge should be parallel to the normal velocity vector for α_{opt}. By crossflow theory, the effective leading-edge angle of attack required to achieve this is

$$\alpha_e = \tan^{-1}(\tan\alpha_{opt}/\cos\Lambda) \tag{21}$$

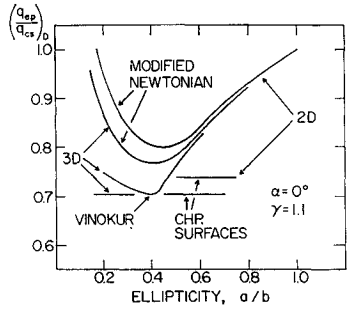

Fig. 3 Heating-rate reduction factors for elliptical surfaces with the same drag.

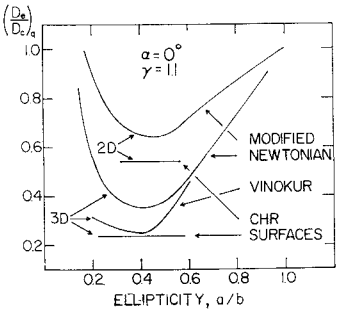

Fig. 4 Drag-reduction factors for elliptical surfaces with the same peak heating rate.

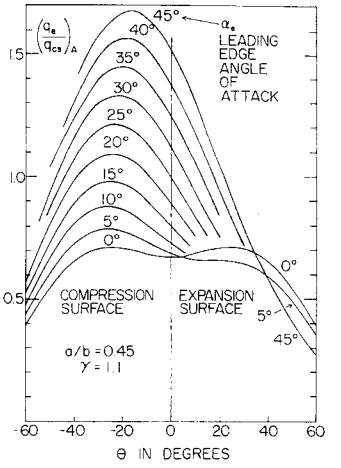

Fig. 5 Heating distributions vs angle of attack for a blunt elliptical leading edge.

For two leading edges at the same sweep, vehicle orientation, and flight conditions, differing only in cross-sectional shape, the influence of sweep cancels when the drag and heating ratios are compared (under the crossflow assumptions). For this assumption, $(q_{ep}/q_{cs})_{D2D}$ and $(D_e/D_c)_{q2D}$ may be used as given in Eqs. (7) and (9).

The vehicle must possess some α modulation capability to allow transient maneuvers at the peak heating point in its trajectory. The heating must thus be studied for α values other than α_{opt}. In this situation the blunt leading edge will not have the stagnation line lying along its line of symmetry. The angle of attack to which the leading edge may be rotated before the local heating rate causes the skin temperature limit to be reached must therefore be determined.

The influence of α variation was found for the optimal elliptical configuration ($a/b = 0.45$), and the results are presented in Fig. 5. Even though the heating advantage of the elliptical leading edge is reduced for off-design α_e values, it is superior to circular cylinders for $\Delta\alpha_e$ transients up to $\pm 16°$ [where $(q_e/q_{cs})_A = 1.0$]. This $\Delta\alpha_e$ range is much in excess of that anticipated in practical situations, hence, elliptical leading edges should retain their superiority over circular leading edges in those cases.

Discussion and Conclusions

General selection criteria have been established for optimizing the leading surfaces of lifting re-entry vehicles for two design situations: 1) minimizing peak heating rate for fixed drag, and 2) minimizing drag for a given peak heating rate. Comparison of Eqs. (7) and (9) and Eqs. (8) and (10) shows that the leading edge or nose that is best by one criterion is the best leading edge or nose by the second criterion, since the right sides of those pairs of equations are powers of each other.

Curves shown for $(q_{ep}/q_{cs})_D$ and $(D_e/D_c)_q$ have definite minima and exhibit variations sufficiently large for the optimal elliptical shapes to be selected precisely. Reductions of 20–23% in $(q_{ep}/q_{cs})_D$ and 36–65% in $(D_e/D_c)_q$ were found for the best elliptical surfaces compared to circular surfaces. Although the advantage of the best elliptical leading-edge shape is somewhat reduced for $\Delta\alpha_e$ transients, these surfaces are still superior to the circular leading edge for practical design situations. Advantages of the best elliptical surfaces are sufficiently great to justify the use of the selection criteria to investigate other families of foresurfaces for lifting orbital re-entry craft.

Elliptical leading surfaces have an additional characteristic to recommend their use. The minima for $(q_{ep}/q_{cs})_D$ and $(D_e/D_c)_q$ occur at nearly the same ellipticity (0.40–0.45) for both noses and leading edges. This fact simplifies design problems on orbital lifting craft using these surfaces in that the same 0.45 elliptical cross section may be chosen for both noses and leading edges. As noted earlier, the shape that is best by one criterion is best by the second. Thus, this single elliptical cross section is optimal for drag reduction or heating-rate reduction for both noses and leading edges. This shape is thus optimal for an intermediate tradeoff as well, giving maximum mission latitude to an orbital lifting re-entry craft with elliptical leading surfaces of this cross section.

References

[1] Hankey, W. L., Jr. and Hooks, L. E., "Constant convective heating rate surfaces for lifting re-entry vehicles," AIAA J. 1, 1533–1536 (1963).

[2] Lees, L., "Laminar heat transfer over blunt nosed bodies at hypersonic flight speeds," Jet Propulsion **26**, 259–269 (April 1956).

[3] Vinokur, M., "Laminar heat-transfer distribution on oblate ellipsoidal noses in hypersonic flow," Inst. Aeron. Sci. **29**, 113–114 (January 1962).